

## Monitoring the Forest Fire with the CINRAD over the Yunnan Plateau

Balin XU<sup>1</sup>, Bing SHU<sup>1</sup>, Yunchang CAO<sup>2\*</sup>, Linghao ZHOU<sup>2,3</sup>, Shuyang XU<sup>1</sup>, Liping LIU<sup>3</sup> and Liyan XIE<sup>1</sup>

<sup>1</sup>Yunnan Meteorological Bureau, Kunming, 650034, China

<sup>2</sup>China Meteorological Observation Center, Beijing, 100081, China

<sup>3</sup>School of Electronic and Information Engineering, Beihang University, Beijing, 100191, China

<sup>4</sup>Chinese Academy of Meteorological Sciences, Beijing, 100081, China

\*Corresponding author: Yunchang CAO, China Meteorological Observation Center, #46 Zhongguancun South Street, Haidian District, Beijing, China, Tel: 8613401198813; E-mail: [caoyc@cma.gov.cn](mailto:caoyc@cma.gov.cn)

### Abstract

In order to explore a new method of forest fire monitoring, the application of new generation C-band weather radar in high mountains is discussed. Using the volume scan data of the new-generation C-band air return radar in Kunming, with quality control methods, echo filtering, and algorithm discrimination, the smoke echo of a suspected forest fire is obtained. The radar's judgment was further verified after the field survey and the use of unmanned aerial vehicles to understand the situation. It was found that the radar monitored the whole fire process, including rising, spreading, and extinguishing. The results show that the new-generation C-band weather radar has a specific ability for forest fire detection and can achieve all-weather monitoring with high sensitivity. Moreover, the location and time of the two fires observed by the radar are accurate, and the time of the fire in Anning has a certain amount of advance compared with the manual monitoring. From the direction of the smoke echo, it is possible to judge the trend of the fire situation on the ground, which is helpful for the accurate research and judgment of the development trend of the fire site, as well as some reference information to determine the location of the embers after the fire. Besides, some scientific data can be provided for post-investigation.

**Keywords:** C-band weather radar; Forest fire; Identification and monitoring; Echo; Plateau and high mountain

### Introduction

A radar operational network composed of over 270 C-band and S-band weather radars has been established by

China Meteorological Administration (CMA) to monitor hazardous weather conditions, which plays a crucial role in disaster prevention and reduction [1]. While detecting severe convective weather, radars can also detect various clutter generated by the smoke dispersion from forest fires into the atmosphere. In recent years, some scholars have conducted research on this topic. For instance, Huang [2] analyzed radar-detected data from ten forest fires in Zhejiang Province. They found that the new-generation S-band weather radar CINRAD/SA can monitor forest fires in Wenzhou. Zhang [3] analyzed radar echo characteristics during a forest fire on January 23, 2015, and an explosion at the Gulei oil depot in Zhangzhou on April 6, 2015. They also found that CINRAD/SA radar can identify smoke echoes from forest fires, urban fires, and explosions and extract some features from these echoes. Huang [4] used radar echo noise filtering methods to effectively eliminate clutter from other sources, which improves the radar warning rate for forest fires. Huang [5] used the CINRAD/SA radar in Wenzhou to detect forest fire echoes for several fire events in 2010. Their approach involved analyzing, processing, and determining the radar base data according to different characteristics of forest fire, precipitation, and clutter echoes. This method achieves forest fire identification and implements a preliminary localization and automatic alarm system. Chen [6] utilized S-band radar with VCP21 precipitation mode in Shanghai to study the radar echo characteristics of smoke from an urban fire in the Minhang District on May 4, 2006. Some radar echo characteristics of this significant fire were obtained and analyzed. Shu [7] monitored transmission line wildfires using the new-generation S-band weather radar network. They pointed out that the clutter echoes are more significant when detecting wildfires at close distances or high altitudes at far distances. Luo [8] applied a storm recognition algorithm for the S-band Doppler weather radar to identify forest fire echoes in Zhejiang Province. They found that the echoes were weak and structurally loose during the early stages and extinction of fires. This leads to false detections due to their mixture of small-scale weak echoes. A significant number of researches using the new-generation S-band weather radar in the eastern coastal regions of China have been carried out to detect forest fire. Note that the new-generation C-band weather radar comprises about half of the total number of radars in China. Studies about using C-band weather radar for forest fire detection have yet to be extensively explored. Compared to the S-band, the new-generation C-band weather radar has higher sensitivity due to shorter wavelengths. However, this also leads to more significant attenuation. The C-band radar provides more precise and closer observations of small-scale convective clouds in the atmosphere, guaranteeing its more sensitivity to smoke echoes from forest fires. CINRAD/CC type weather radar is a full-polarization, multi-Doppler new-generation C-band weather radar used by the CMA for meteorological operations. It primarily deploys in the western mountainous regions of China. Xu [9] preliminarily analyzed the ability of C-band high-altitude weather radar to detect forest fires. Their results suggest that high-altitude C-band radar may also have some potential in detecting forest fires. Afterward, they further summarized the forest fire characteristic echoes of the C-band weather radar during three forest fires in Yunnan. Based on previous studies, they developed a preliminary warning system [10]. However, high-altitude radar should have performed more while detecting low-level echoes in conventional operational scan modes. Xu [11] once pointed out that ultra-low elevation scans can improve low-level echo detection capability for high-altitude radar. Based on the above-mentioned previous research using the new generation S-band weather radar, this study combines the characteristics of high-altitude radar in Yunnan Province. It utilizes data from the high-altitude new-generation C-band weather radar in Kunming to conduct a more in-depth

case analysis of a forest fire's occurrence, development, and extinction.

## Data and Quality Control Methods

The radar base data of the new-generation C-band weather radar used in this study are provided by the operational department of CMA. The data are primarily from Kunming's CINRAD/CC (3830) radar set. It is an entirely coherent pulse Doppler radar with high transmission power, narrow beam width, high antenna gain, wide pulse width, high receiving sensitivity, and extensive dynamic range. Apart from this, some individually distributed high-altitude radars, which have been continuously operated as part of the national meteorological operational network, are also utilized in this study. The standard VCP precipitation observation mode is selected to guarantee consistent radar data format and detection modes. The radar basis data are spatially stored in polar coordinates and temporally sampled at approximately 6-minute intervals in continuous volume scans. The radar data are scanned every 14 elevation angles, and each elevation scan has 512 radial beams with 500 range bins spaced at 300-meter intervals for each beam. A total amount of 500 data points is stored for each range bin for  $Z$  (reflectivity),  $V$  (radial velocity), and  $W$  (spectrum width), respectively. The observed raw data files record data from 1 to 14 elevation angles in polar coordinates, arranged in the order of intensity, radial velocity, and spectrum width. The data are stored from the lowest to the highest elevation. Each elevation angle and radial beam contains 512 data points for each element. The Kunming radar station is located at longitude  $102.57^\circ\text{E}$  and latitude  $25.05^\circ\text{N}$  with an antenna elevation of 2484.5 meters. Forest fire case data was collected from local forest fire prevention and control agencies. To ensure the quality of the radar data, pre-processing and quality control procedures were conducted before further investigation. First, the radar reflectivity volume scan data in polar coordinates were transformed into a unified Cartesian coordinate grid. Subsequently, conventional methods are applied to filter out clutter, super-refracted, second, and ground echoes, and perform nine-point smoothing to ensure data quality. Afterward, the station-based data were interpolated into a grid format, and various algorithms were applied for further analysis and interpretation.

## Principles of Radar Echo Generation from Forest Fire

### Basic Principles of Radar Echo Generation from Forest Fire

Radar echoes from forest fires are primarily generated by suspended particles in the air caused by forest conflagrations and fire explosions, such as leaves and branches. Additionally, atmospheric updraft changes and turbulence from forest fires can contribute to radar echoes. It is believed that both of these mechanisms generally coexist. When a forest fire occurs, the radar electromagnetic waves are scattered because of the burning branches, leaves, or other materials with conductive properties, which constitute the main factor for backward radar scattering. According to the definition of radar echo intensity (reflectivity), radar reflectivity  $Z$  is related to the distribution  $N(D)$  of hydrometeors in a unit volume and the diameter  $D$  of the hydrometeors.  $Z$  is equal to the sum of the sixth power of the diameters of all scattering particles in the effective illuminated volume, given by:

$$Z = \int_0^{\infty} N(D)D^6 dD$$

Where  $Z$  is measured in  $\text{mm}^6/\text{m}^3$ ,  $N(D)$  is the droplet size distribution function representing the number

of particles with diameters between  $D$  and  $D + dD$  in a unit volume. It can be seen that the radar reflectivity  $Z$  is primarily determined by the diameter  $D$  of the detected particles. The principle of detecting forest fires with radar is similar to detecting precipitation particles. Radar emits electromagnetic waves that encounter airborne dust generated by the thermal uplift of burning fires. This further contributes to the backward scattering and forms radar echoes. According to the basic principles of the radar equation, radar is less sensitive to small-diameter smoke particles but more sensitive to larger ones. Fire smoke is not large enough to generate strong radar echoes. The primary contribution to strong radar echoes is the backward scattering from larger particles, such as ash from burning branches and leaves lifted by the heat of the fire. Together with the effects of the first mechanism, these factors generally result in observable radar echoes. In addition, atmospheric turbulence generated by ongoing combustion can lead to radar echoes. It is generally believed that these two scattering mechanisms coexist when detecting forest fire echoes with radar. The first mechanism typically dominates, while the role of turbulence-induced echoes is negligible during the early stages of an explosion or above the fire's convective column. After the explosion, the dilution of particle concentration and the fall of larger particles, coupled with ongoing high-temperature gradients inducing turbulence, make the second mechanism more significant. This phenomenon also happens when the forest fire is downwind from the convection column. Together with the first mechanism, weaker echoes are produced. It tends to develop rapidly when a forest fire occurs with suitable weather conditions (e.g., clear sky or dry conditions). The forest fire creates local high temperatures on the ground and generates a thermal convection column. This lift burning and partially burned leaves, small branches, and other materials to higher altitudes. Once these materials reach the minimum altitude detectable by the radar, the observable radar echoes can be detected. Atmospheric turbulence scattering of electromagnetic waves has been extensively researched from theory to experimentation [11]. Turbulence scattering echoes exhibit characteristics similar to precipitation echoes, which present the characteristic of diffuse targets [12]. The equivalent reflectivity factor for turbulence scattering (denoted as  $Z_{et}$ ) is introduced to describe its scattering capability. Turbulence scattering can be regarded as a diffuse target, and the radar meteorological equation for diffuse targets is given by:

$$Z_{et} = \frac{1024 \ln 2}{|k|^2 \pi^3} \times \left( \frac{\lambda^2 P_r}{P_t G_e^2 f_c \theta^2} \right) R^2$$

$$|k|^2 = \left| \frac{M^2 - 1}{M^2 + 1} \right|^2$$

where  $Z_{et}$  is the reflectivity factor for turbulence scattering in  $\text{mm}^6/\text{m}^3$ ,  $k$  is the complex refractive index of water associated with the refractive index, usually taking the index of water  $M$  as 0.93 for water droplets,  $\lambda$  is the wavelength,  $P_r$  is the radar power,  $P_t$  is the pulse power,  $G_e$  is the antenna effective gain after accounting for antenna losses,  $f_c$  is the pulse width,  $\theta$  is the antenna beam width, and  $R$  is the radar detection distance [13]. Note that turbulent scattering is also related to the radar structure constant  $C_n$ .  $Z_{et}$  is generally weak, ranging from -40 dBZ to 10 dBZ. Previous studies have indicated that radar can observe widespread turbulence echoes within the low atmosphere for coastal regions during the warm and humid season [14]. The radar receives echoes from partially burned particles lifted by fires that can be electromagnetically polarized. These suspended materials in a forest fire are typically of larger sizes and irregular shapes, such as small

branches (elongated) or leaves (planar) [15]. These specific forms differ from the typical spherical-objects assumption in the radar equation. This makes the calculation of their backward scattering cross-section highly complex. To quantify these characteristics, extensive experiments are required. It is generally considered that echoes from such scenarios produce strong intensity and contribute significantly to forest fire radar echoes, whereas echoes generated by turbulence scattering are relatively weaker.

### **Conventional Methods for Extracting Forest Fire Radar Echoes and Special Measures in Plateau Regions**

Various factors in the atmosphere can generate radar echoes, including raindrop precipitation, clear-sky echoes, ground clutter, super-refraction echoes, point clutter from aircraft and birds, secondary echoes from radar wave reflections, etc. Based on the distinct characteristics of different types of echoes in radar observations, conventional methods are employed to filter clear-sky, super-refraction, ground clutter, secondary, and precipitation echoes. These filtering methods proposed in previous studies are systematically applied in this study. Afterward, the remaining echoes can be preliminarily identified as potential forest fire echoes.

Considering the unique characteristics of plateau regions, such as terrain variation within small-scale and higher altitudes for radar installation, several special measures are adopted:

- Radars in the western region are often set on high mountaintops with significant differences in altitude among different radars. To account for the varying altitudes, specific identification thresholds are set for different altitudes to ensure adequate vertical coverage.
- Given the significant influence of local wind patterns in high-altitude mountainous regions, forest fire echoes tend to exhibit specific upward characteristics. Thus, the identification of velocity fields is introduced.
- A two-step filtering approach is employed to effectively eliminate echoes from localized, small-scale cloud clusters due to the prevalence of convective precipitation in high-altitude plateau areas.

Through these steps, preliminary identification of forest fire echoes suitable for plateau regions can be obtained. Afterward, human judgment was conducted to determine the fire-related smoke echoes fundamentally. Conventional echo filtering methods have been extensively discussed in previous literature. At the same time, these extraordinary measures primarily consider factors such as the altitude of the forest fire echo top, thickness, and the high-altitude radar installation location. By simultaneously considering wind direction and velocity from ground-based automatic meteorological stations and radar-observed velocity fields, features such as echo movement direction can be comprehensively analyzed, and it is possible to determine whether an echo is associated with fire. Finally, recent forest fire evolution case studies monitored by seven C-band new-generation weather radars in Yunnan will be further analyzed, and discernment thresholds can be extracted and applied for validation.

### **Case study for Evaluating Kunming Radar**

A specific observation dataset from the Kunming radar was selected for a case study using the abovementioned methods.

### General Description of the Forest Fire Incident

On May 9th at 15:33, a forest fire occurred at Shanshenba, Kunming, Yunnan Province, China. Influenced by factors such as high temperatures, strong winds, and combustible vegetation, the fire exhibited multiple instances of spotting and created several fire lines. One of the fire lines extends northward into Lufeng County, Chuxiong Prefecture. By May 12th at 12:00, the open flames in the fire area were extinguished, and by 1:10 a.m. on May 14th, the fire was fully under control. The total burned area of this forest fire was 170.1 hectares (110 hectares in Anning District and 60.1 hectares in Lufeng District). The firefighting efforts involved nearly 5,800 personnel.

### Initial Fire Situation Monitored in Lufeng County by Kunming Radar

The initial fire situation was analyzed using the echo data from the Kunming radar. **Figure 1** shows the data obtained after filtering out non-forest fire echoes on May 9, 2020, using the abovementioned methods. The radar echo image at 12:35 (**Figure 1(a)**) reveals isolated point-like fire echoes concentrated in the southeastern part of Lufeng County. This triggers the software's alarm's activation and preliminarily identifies a suspected smoke echo area of approximately 9.54 km<sup>2</sup> at coordinates 102.0812°E, 25.0891°N. In the radar echo image at 12:59 (**Figure 1(b)**), more detected fire smoke echoes covered an area of about 25.78 km<sup>2</sup>, extending into the airspace near the border with Anning City. Given that the prevailing wind direction during this season in Yunnan is from the southwest, a local northwest wind suggests a potential risk to the south of the fire area. By 14:21 (**Figure 1c**), no fire smoke echoes were observed within the Anning City area.



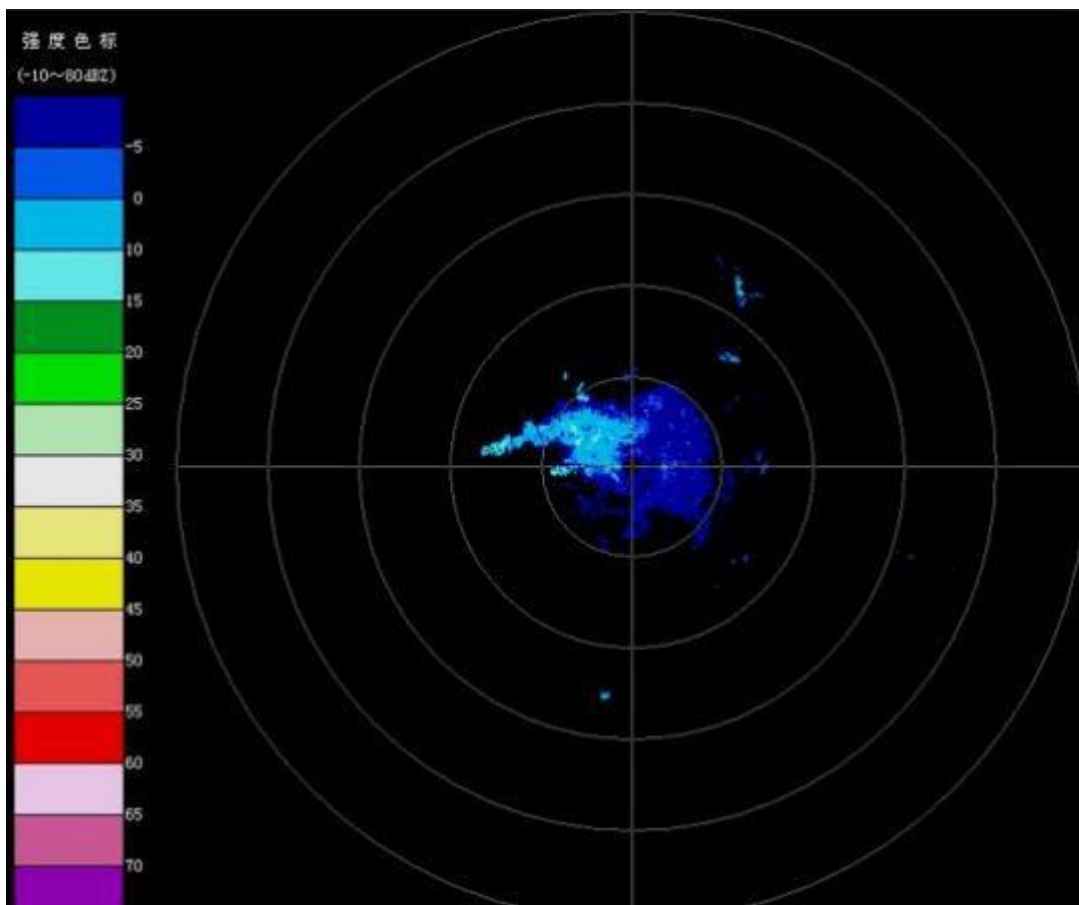


**Figure 1:**Initial situation of fire in Lufeng County monitored by Kunming Radar.

After conducting on-site investigations, the analyzing results detected by radar observations mentioned above were largely confirmed. This proves that the new- generation C-band weather radar has a specific capability for detecting forest fires and possesses higher sensitivity.

**Initial Fire Situation Monitored in Anning City by Kunming Radar**

It was shown that until 15:20 and 15:26 on May 9, 2020, point-like fire echoes were identified within the vicinity of Anning City through radar echo images. The detected area was concentrated approximately 21 kilometers southeast of Lufeng County, as shown in **Figure 2**. **Figure 2(a)** illustrates the radar echo intensity, while Figure 2(b) depicts the radar echo velocity. By extracting fire echoes, the initial detection was made at the location marked by the black arrow with the marker "A" in the radar echo image at 15:20 (**Figure 2(c)**). This finding was further corroborated by the radar echo image at 15:26 (**Figure 2(d)**). Notable features were also observed in the velocity field, and introducing velocity field indicators was proved to have a specific effect on enhancing forest fire detection. The suspected smoke echo area was approximately 7.44 km<sup>2</sup>, with coordinates 102.2173°E, 25.01727°N. The radar's detection of fire echoes within Anning City preceded manual alerts by approximately 13 minutes.





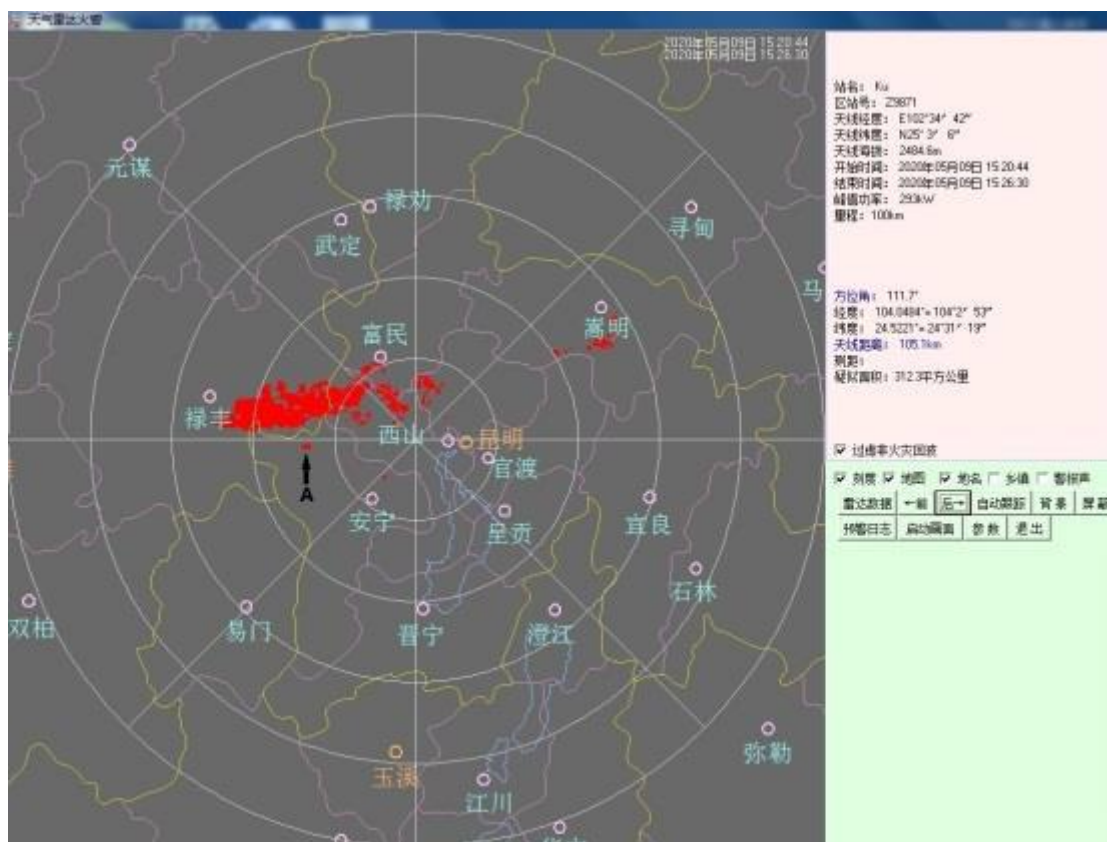
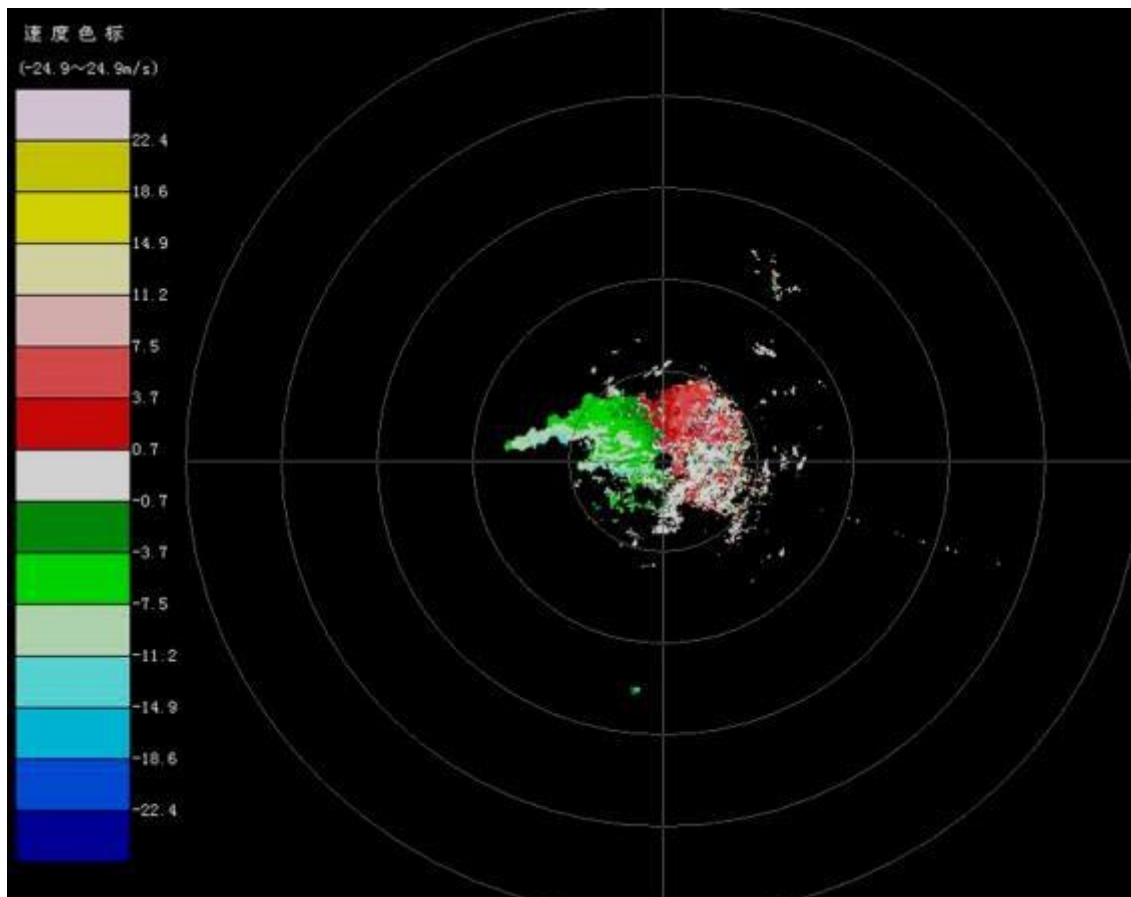




**Figure 2:** Radar fire alarm diagram of Kunming at 15:20 and 15.26 on May 9, 2020.

The satellite heat source monitoring of Yunnan Ecological Meteorology and Satellite Remote Sensing Center further verified the sequence of the two fires in Lufeng and Anning. This case analysis shows that in terms of timeliness, radar monitoring has fewer blind areas, which has advantages in time and space compared with artificial video field monitoring. It is also possible to detect forest fires in advance. Moreover, the monitoring distance is about 100 km, and the monitoring area can be reached in 6 minutes. There were similar cases of early detection in several other cases.

#### **Fire development situation monitored by Kunming Radar**

The two fires developed further in the next half hour after the fire initiation, and the air dust echoed, as shown in **Figure 3**. The fire development is relatively vigorous at this time, and the echo area of dust in the air reaches 572.76 km<sup>2</sup>. Although the smoke of the two fires in **Figure 3(a)** is relatively chaotic, the location of the fire point is still precise. The smoke of the two fires in **Figure 3a** is relatively regular, and the trend is clear. The trend of smoke and dust in the figure can deduce the fire trend on the ground, which should be helpful information for the ground organization for firefighting and provide more timely and comprehensive reference information for the command and decision of the rescue.

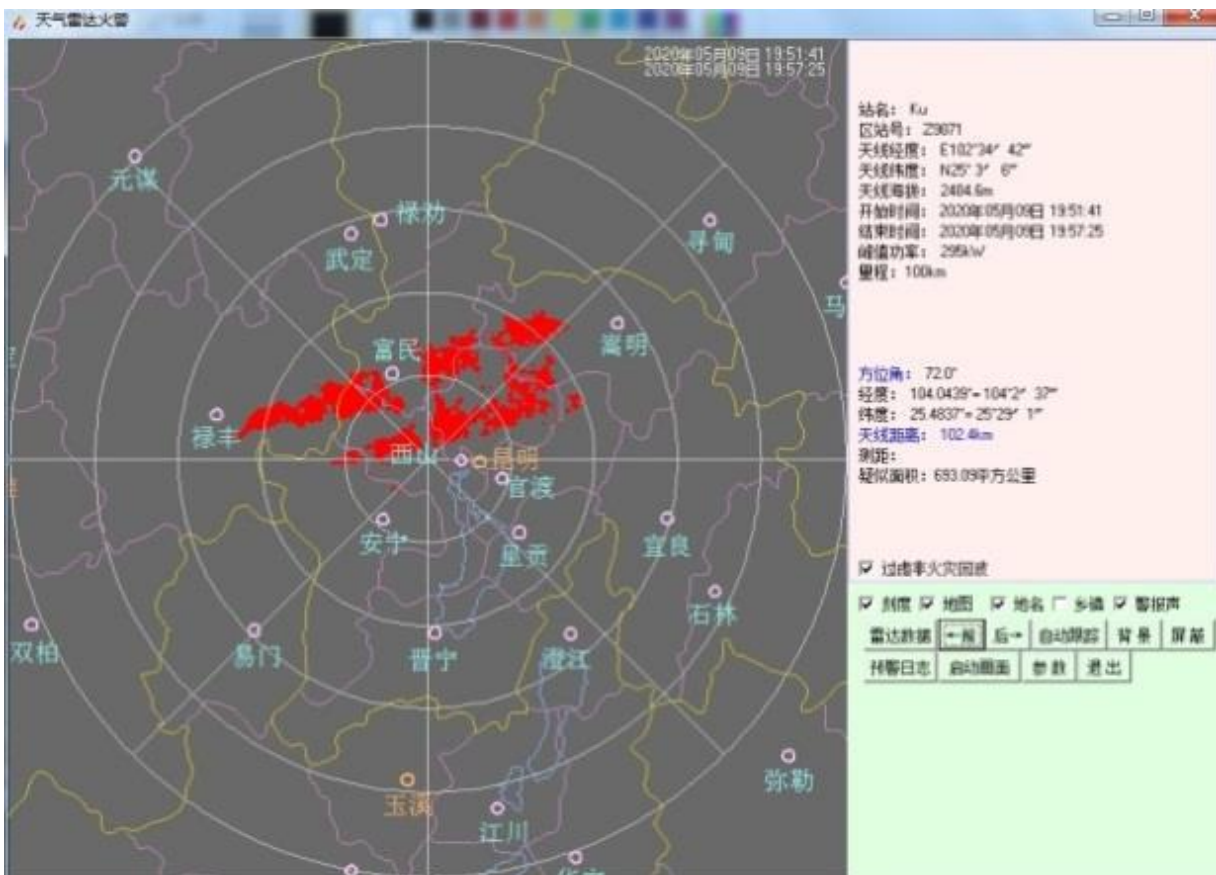


**Figure 3:** Radar fire alarm diagram of Kunming at 16:07 and 19:51 on May 9, 2020.

### Later Stage situation of the fire monitored by Kunming Radar

By 17:33 on the 12th day, the fire had been weakened, as shown in **Figure 4(a)**. Lingering flames remain at the border between Anning and Lufeng counties, particularly on the side of Lufeng County. The fire in Anning City had likely been extinguished, as no smoke echoes were detected in multiple subsequent volume scans. At 01:54 on the 13th day, the remaining flames further diminished and were nearing complete extinguishment, as depicted in **Figure 4(b)**. The remaining flames' exact locations were visible at coordinate's 102.3009°E 25.0813°N. This information can also provide some reference for identifying the locations of lingering flames and cleaning up the fire area. Moreover, it can offer valuable scientific data support for post-fire investigations related to forest fires.





**Figure 4:** Radar fire alarm diagram of Kunming at 17:33 on May 12 and 01:54 on May 13, 2020.

### Further Verification of Post-Fire Conditions by Field Surveys and Drone Usage

Drones were deployed for on-site field surveys to gain a deeper understanding and validate the radar observations after the fire, as depicted in **Figure 5**. These on-site investigations found that the ignition point's positioning was relatively accurate, and the areas affected by the fire were consistent with the trends observed in the radar-detected smoke and dust plumes during the fire.



**Figure 5:** Pictures taken by Unmanned Aerial Vehicle and corresponding geographical positions.

## Conclusion

By analyzing the data from two forest fire incidents monitored by the Kunming radar and subsequently conducting on-site field surveys and using drones to assess the post-fire conditions, the radar analysis results have been verified in conjunction with data from ground automatic weather stations. Based on these findings and analysis of other cases, the following preliminary conclusions can be drawn:

- The analysis demonstrates that the new generation C-band weather radar also possesses a specific capability for detecting forest fires. Timely and accurate radar monitoring can provide technical support for early warnings and firefighting efforts.
- Analyzing the radar echoes generated by the forest fire case indicates that the radar captured the entire process of ignition, plume rising, expansion, and extinguishing. Radar monitoring is continuous and can detect the ignition early and provide early warnings. Moreover, the radar exhibits high sensitivity and accurate distance resolution in its detection capabilities.
- The analysis of the smoke dispersion during the fire development process allows for assessing ground fire trends and provides comprehensive and timely reference information for firefighting coordination.
- In the later stages of the fire, the radar can offer reference information for identifying residual fire locations and aiding in post-fire investigations.
- The analysis also reveals that for Yunnan's high-altitude mountain radars, the long-distance detection ability of forest fire echoes is weakened due to the high detection altitude. Using ultra-low elevation angle scanning can enhance the long-distance echo detection capability.

The rugged terrain and extensive forest coverage in Yunnan inherently pose challenges for fire monitoring. Utilizing a 6-minute frequent weather radar scan can enhance monitoring capabilities to a certain extent. Similar results have been observed in various cases. However, this particular incident exhibited favorable monitoring conditions. The study also identified relatively high false alarm rates in some instances, especially in urban areas and large factories. Moreover, the false alarm rate tends to be higher in the afternoon compared to the morning. Further research and case analysis are required to improve the operational capabilities in practice.

## References

1. [Chen YL, Cao XG, Shao LL, et al. A Research on the Radar Echoes of a Severe Fire Smoke in Shanghai. J Meteorological Sci. 2010;30\(1\):121-5.](#)
2. [Ge RS, Zhu XY, Jiang HY. A method for improving the probing ability of Doppler Weather radar in the clear air. J App Meteorological Sci. 2000;11\(3\): 257-63.](#)
3. [Gossard EE, Strauch RG. Radar Observation of Clear Air and Clouds. Amsterdam: Elsevier, 1983.](#)
4. [Han L, Wang HQ, Tang XG, et al. Review on Development of Radar-based Storm Identification, Tracking and Forecasting. Meteorol. 2007;1: 3-10.](#)
5. [Huang KH, Zhang DY, He J, et al. Forest fires observations by using the new Doppler weather radar. Forestry Sci Technol. 2007a;32\(5\):33-36.](#)
6. [Huang KH, Zhou GT, Xie HH, et al. Forest fires Detected by using CINRAD/SA Radar. J](#)

- [Meteorological Sci. 2007b;27\(S1\):99-106.](#)
7. [Huang KH, Zhu J, Huang YP, et al. Fire Automatic Detection System Based on Doppler Weather Radar. Meteorology. 2013; 39\(2\): 241-8.](#)
  8. [Luo H, Zhang J, Zhu KY, et al. Storm cell identification algorithm to identify forest fire. Fire Safety Sci. 2014; 23\(4\): 218-24.](#)
  9. [Shu SW, Zhang SW, Xu J. Study on automatic identification algorithm of wild fire near transmission lines based on CINRAD-NET. Proceedings CSEE. 2020;40\(13\): 4200-9.](#)
  10. [Wang B, Xu Y, Bi B. Forecasting and warning of tropical cyclones in China. Data Sci J, 2007;6: S723-S737.](#)
  11. [Xu BL, Yang WJ, Xu SY, et al. Preliminary Analysis of the Ability of C- Band Mountaintop Radars to Detecting Forest Fires. Meteorology. 2020a;46\(8\):1113-21.](#)
  12. [Xu BL, Xie LY, Lu P, et al. Warning system of C-band Weather Radar to Detect Forest Fires in Yunnan. J Catastrophogy. 2020b;35\(3\):125-30.](#)
  13. [Xu BL, Liu LP, Xu WJ, et al. Improved Detection Using Negative Elevation Angles for Mountaintop Radars. Meteorology. 2008;34\(9\):28-33.](#)
  14. [Yu XD, Yao XP, Xiong TN, et al. Doppler Weather Radar Principle and Business Application Beijing. China Meteorological Press. 2006;220-9.](#)
  15. [Zhang SS, Wei M, Lai QZ, et al. Analysis of CINRAD echo characteristics about two fires. J Meteorological Sci. 2017;37\(3\):359-67.](#)

### **Citation of this Article**

XU B, SHU B, CAO Y, ZHOU L, XU S, LIU L and XIE L. Monitoring the Forest Fire with the CINRAD over the Yunnan Plateau. Mega J Case Rep. 2023;6(9):2001-2015.

### **Copyright**

© 2023 CAO Y. This is an open-access article distributed under the terms of the [Creative Commons Attribution License \(CC BY\)](#). The use, distribution or reproduction in other forums is permitted, provided the original author(s) or licensor are credited and that the original publication in this journal is cited, in accordance with accepted academic practice. No use, distribution or reproduction is permitted which does not comply with these terms.